

**DESIGN AND IMPLEMENTATION OF LIQUID-
BASED FINE-TUNABLE SOLENOID MEMS
INDUCTOR**

AHMAD HAFIZ BIN MOHAMAD RAZY

UNIVERSITI SAINS MALAYSIA

2018

**DESIGN AND IMPLEMENTATION OF LIQUID-BASED FINE-TUNABLE
SOLENOID MEMS INDUCTOR**

by

AHMAD HAFIZ BIN MOHAMAD RAZY

**Thesis submitted in fulfilment of the
requirements for the degree of
Master of Science**

April 2018

ACKNOWLEDGMENT

First and foremost I would like to pay a heartfelt tribute to some of the parties who had let me gain a knowledge and experience during my postgraduate research project implementation. There are individuals who assisted and helped me, directly or indirectly during my research projects designation. I would like to take this opportunity to show my deepest gratitude to all of them.

First of all, I would like to thank Dr Mohd Tafir Bin Mustaffa for guiding me to accomplish my postgraduate research project. I am grateful to my supervisor for his encouragement, permission and approval during my project designation. Special thanks to Assoc. Prof. Dr Asrulnizam Bin Abd Manaf for his hospitality extended to me. He gave me a lot of guidance and willing to share his experience with me.

Next, I would like to express my deepest gratitude to my guidance, Dr Farshad and Dr Fatemeh. They encourages me and provides me many opinions during project designation and implementation. My gratitude also goes to the staff from CEDEC for the technical supports on the network analyzer provided.

Last but not least, my thanks go to my family members who offered me unlimited moral support. Without them, I can never complete my research project successfully. A word also goes to those who inevitably forgot to mention. I am no less grateful to them and I hope that they will forgive my oversight.

TABLE OF CONTENTS

	Page
ACKNOWLEDGEMENT	ii
TABLE OF CONTENTS	iii
LIST OF TABLES	viii
LIST OF FIGURES	x
LIST OF ABBREVIATIONS	xvi
ABSTRAK	xviii
ABSTRACT	xix
CHAPTER ONE – INTRODUCTION	
1.1 Introduction of Research	1
1.2 Problem Statement	3
1.3 Objectives	5
1.4 Scope of Work	5
1.5 Thesis Outline	6
CHAPTER TWO – LITERATURE REVIEW	
2.1 Introduction	8
2.2 Types of Inductor	9
2.3 Analytical Modelling of Integrated Inductor	11
2.3.1 Model of the Planar Spiral Integrated Inductor	11
2.3.2 Series Resistance Loss	13
2.3.3 Substrate Loss and Self-resonance Factor	14

2.4	Methods to Enhance Quality Factor	17
2.4.1	Width of Conductor	18
2.4.2	Size of Inner Turns of the Inductor Coils	20
2.4.3	Gap Distance between Segments of Winding	21
2.4.4	Inductor on Oxide Layer (SOI Wafer)	23
2.4.5	Substrate Thickness	24
2.4.6	Liquid-based Inductor	25
2.5	Methods of Tuning the MEMS Inductor	28
2.5.1	Ferrofluid-based Variable Solenoid Inductor with Micro-pipe	28
2.5.2	MEMS Variable Solenoid Micro-fluidic Inductor with Galinstan-based	29
2.5.3	Stretchable Inductor with Liquid Metal Galinstan	31
2.5.4	Ferrofluid-based Variable Planar Inductor with Actuation Coil	33
2.5.5	On-chip Liquid Micro-variable Inductor	35
2.6	Summary	38

CHAPTER THREE – METHODOLOGY

3.1	Introduction	42
3.2	Integrated Fine-tunable Solenoid MEMS Inductor Design Methodology	46
3.2.1	Selection of Structural and Design Dimensions	46
3.2.2	Design of the Integrated Fine-tunable Solenoid MEMS Inductor for 2.4 GHz Applications	51

3.2.3	Optimisation of the Integrated Fine-tunable Solenoid MEMS Inductor for Proof-of-Concept	62
3.3	Methodology of the Fabrication Process	67
3.3.1	Wafer Dicing	68
3.3.2	Sample Cleaning	69
3.3.3	Metal Deposition	70
3.3.4	Annealing	72
3.3.5	Laser Patterning	73
3.3.6	Plasma Cleaning	76
3.3.7	Wire Bonding	77
3.4	Summary	79

CHAPTER FOUR – RESULTS AND DISCUSSIONS

4.1	Introduction	81
4.2	Simulation Results of the Integrated Fine-tunable Solenoid MEMS Inductor at 2.4 GHz	82
4.2.1	Simulation Results for Ferrofluid-based Inductor with $\mu_r=1.3$	82
4.2.2	Simulation Results for Ferrofluid-based Inductor with $\mu_r=3.1$	85
4.2.3	Simulation Results for Ferrofluid-based Inductor with $\mu_r=5.4$	88
4.3	Simulation and Measured Results of the Integrated Fine-tunable Solenoid MEMS Inductor at 400 MHz	93
4.3.1	Simulation Results of the Integrated Fine-tunable	93

	Solenoid MEMS Inductor at 400 MHz	
4.3.2	Measurement Results of the Integrated Fine-tunable Solenoid MEMS Inductor at 400 MHz	97
4.3.2(a)	Measured Results of the 400 MHz Design Inductor	97
4.3.2(b)	Comparison between Simulations and Measured Results of the 400 MHz Design Inductor	100
4.4	Discussions on the Simulation and Measured Results for the 400 MHz Design Inductor	103
4.5	Summary	107
 CHAPTER FIVE – CONCLUSIONS AND FUTURE WORKS		
5.1	Conclusions	108
5.2	Future Works	109
 REFERENCES		110
 APPENDICES		
Appendix A: Fully Automatic Dicing Saw Machine		
Appendix B: Auto RF Sputter Coater		
Appendix C: Furnace Oven		
Appendix D: Laser Micromachining Rapidx 250		
Appendix E: Wire Bonder Machine		
Appendix F: S-Parameters Value in Simulation and Measured Results		
F.1	The Conversion of S-Parameters to Y-Parameters	

F.2 Quality Factor and Inductance Value Equations in
Y-Parameters Expression

Appendix G: Measurement Setup

Appendix H: Table of the Parameters Conversion

Appendix I: The Simplification of Y-Parameters using Differential Method

LIST OF PUBLICATIONS

LIST OF TABLES

		Page
Table 2.1	Performances comparison for MMIC and MEMS inductor	11
Table 2.2	Comparison of quality factor with different conductor width (Weon <i>et al.</i> , 2005)	19
Table 2.3	Performances comparison of different enhancement methods for quality factor	27
Table 2.4	Performances comparison of tuning range with different tuning methods	37
Table 2.5	Performances comparison with related references	39
Table 3.1	Specifications of the fine-tunable MEMS inductor	43
Table 3.2	Optimised parameters of the inductor at 2.4 GHz	52
Table 3.3	Parameters of coplanar waveguide	56
Table 3.4	Comparison of the specifications for 400 MHz and 2.4 GHz	63
Table 3.5	Modification of the inductor for 400 MHz	66
Table 4.1	Performances of quality factor and inductance values for difference levels of injection with ferrofluid-based type EMG 911 11 mT at 2.4 GHz	85
Table 4.2	Performances of quality factor and inductance values for difference levels of injection with ferrofluid-based type EMG 905 440 mT at 2.4 GHz	88
Table 4.3	Performances of quality factor and inductance values for difference levels of injection with ferrofluid-based type EMG 901 660 mT at 2.4 GHz	91

Table 4.4	Performances comparison for three types of ferrofluid	92
Table 4.5	Performances of quality factor and inductance values for difference levels of injection (400 MHz design simulation)	96
Table 4.6	Performances of quality factor and inductance values at empty channel (0%) and fully-injected channel (100%) for measured inductor	99
Table 4.7	Performances of quality factor and inductance values at empty channel (0%) and fully-injected channel (100%) for 6 design inductors	100
Table 4.8	Performances comparison between simulations and measured results of the 400 MHz design inductor	102
Table F.1	S-parameters to H-parameters conversion chart (Jamal Deen <i>et al.</i> , 2002)	
Table F.2	H-parameters to Y-parameters conversion chart (Frickey, 1994)	
Table H.1	Equations for the conversion between S-parameters and Z, Y, h, and ABCD parameters with source impedance Z_{01} and load impedance Z_{02}	

LIST OF FIGURES

		Page
Figure 1.1	Silicon-embedded toroidal MEMS inductor (Yu <i>et al.</i> , 2014)	2
Figure 1.2	Solenoid MEMS inductor (Seok <i>et al.</i> , 2001)	3
Figure 2.1	Types of inductor (a) Arc-shaped solenoid inductor (b) Meander inductor (c) Flexible spiral inductor (Chomnawang <i>et al.</i> , 2001; Huang <i>et al.</i> , 2010; Zheng <i>et al.</i> , 2013)	10
Figure 2.2	General model of the planar spiral inductor (Passos, 2013)	12
Figure 2.3	π model of silicon substrate (Passos, 2013)	13
Figure 2.4	Extracted resistance, R_p and capacitance, C_p from π model of a silicon substrate	15
Figure 2.5	Rectangular conductor with a resistance in the direction of L (Rogers <i>et al.</i> , 2010)	19
Figure 2.6	The magnetic fields associated with induced current around the coils (Bahl, 2003; Passos, 2013)	20
Figure 2.7	The SRF of the inductance value and quality factor (a) The SRF of the inductance value (b) The SRF of the quality factor (Passos, 2013)	22
Figure 2.8	Close view of the space between segments of winding (Banitorfian <i>et al.</i> , 2014)	23
Figure 2.9	Before and after the back grinding substrate wafer	25
Figure 2.10	Ferrofluid-based variable solenoid inductor with micro-pipe (Banitorfian, 2016)	29

Figure 2.11	3D view of the (a) cavity on the silicon substrate, (b) deposition of the bottom half of solenoid coil, (c) filling cavity with photoresist for creating channel, (d) deposition of the top half of solenoid coil and removing photoresist, (e) cover the channel with PDMS (Banitorfian <i>et al.</i> , 2015)	30
Figure 2.12	(a) Bottom, (b) top and (c) top side of double planar coil inductor filled with galinstan-based (Lazarus <i>et al.</i> , 2014)	32
Figure 2.13	Tensile strain test of the double planar coil inductor for (a) 0% and (b) 100% (Lazarus <i>et al.</i> , 2014)	33
Figure 2.14	Ferrofluid-based variable planar inductor with actuation coil (Assadsangabi <i>et al.</i> , 2012)	34
Figure 2.15	The illustrations of the ferrofluid motion (a) without bias field effect (b) with bias field effect (Assadsangabi <i>et al.</i> , 2012)	35
Figure 2.16	The dual circular coil inductor (Gmati <i>et al.</i> , 2011)	36
Figure 2.17	The position of the saturated salt water on the dual circular coil inductor (Gmati <i>et al.</i> , 2011)	37
Figure 3.1	Flow chart of the design methodology for the fine-tunable MEMS inductor	44
Figure 3.2	Model of the integrated fine-tunable solenoid MEMS solenoid inductor	46
Figure 3.3	Top view of the integrated fine-tunable solenoid MEMS inductor	47

Figure 3.4	Thickness of the three main layers (aluminium/ SiO ₂ /substrate) (a) Full view of the three main layers (b) Close view of the aluminium and SiO ₂ layers	49
Figure 3.5	The dimensions of the micro-tube	50
Figure 3.6	Length and width of the metal lines	53
Figure 3.7	Dimension of the silicon substrate and SiO ₂	54
Figure 3.8	Ground traces for close loop condition	55
Figure 3.9	Coplanar waveguide cross-section	55
Figure 3.10	The width of the metal trace and ground spacing	56
Figure 3.11	Micro-tube placed at the centre of the inductor with ferrofluid inside of the channel	57
Figure 3.12	Gold wire for upper-half of the inductor	58
Figure 3.13	Wave port for the input and output signal of inductor	60
Figure 3.14	Air-box for radiation boundaries	61
Figure 3.15	Dimension of silicon substrate and SiO ₂ with aluminium patterned on top of SiO ₂	64
Figure 3.16	Full design of the fine-tunable solenoid MEMS inductor at 400 MHz for proof-of-concept	65
Figure 3.17	Flow chart of the fabrication process	67
Figure 3.18	Samples of SOI wafer after wafer dicing process	69
Figure 3.19	Sputtering process of metal deposition	71
Figure 3.20	Aluminium metal deposited on SOI sample	72
Figure 3.21	Annealing process	73
Figure 3.22	Inductor designed on AutoCAD software	75
Figure 3.23	Laser patterning process using laser micromachining	75

Figure 3.24	Process of plasma cleaning using oxygen	77
Figure 3.25	The ball bonding technique of wire bonding process	78
Figure 3.26	Gold wire bonding from first metal line to second metal line	79
Figure 4.1	Quality factor from empty channel (0%) to fully-injected channel (100%) at 2.4 GHz with ferrofluid-based type EMG 911 11 Mt	83
Figure 4.2	Inductance values from empty channel (0%) to fully-injected channel (100%) at 2.4 GHz with ferrofluid-based type EMG 911 11 mT	83
Figure 4.3	Tuning range at 2.4 GHz with ferrofluid-based type EMG 911 11 mT	84
Figure 4.4	Quality factor from empty channel (0%) to fully-injected channel (100%) at 2.4 GHz with ferrofluid-based type EMG 905 440 mT	86
Figure 4.5	Inductance values from empty channel (0%) to fully-injected channel (100%) at 2.4 GHz with ferrofluid-based type EMG 905 440 mT	86
Figure 4.6	Tuning range at 2.4 GHz with ferrofluid-based type EMG 905 440 mT	87
Figure 4.7	Quality factor from empty channel (0%) to fully-injected channel (100%) at 2.4 GHz with ferrofluid-based type EMG 901 660 mT	89
Figure 4.8	Inductance values from empty channel (0%) to fully-injected channel (100%) at 2.4 GHz with ferrofluid-based type EMG 901 660 mT	89

Figure 4.9	Tuning range at 2.4 GHz with ferrofluid-based type EMG 901 660 mT	90
Figure 4.10	(a) Full view and (b) close view of the quality factor from empty channel (0%) to fully-injected channel (100%) for 400 MHz design simulation	94
Figure 4.11	Inductance values from empty channel (0%) to fully-injected channel (100%) for 400 MHz design simulation	95
Figure 4.12	Tuning range of the 400 MHz design simulation	95
Figure 4.13	Quality factor at empty channel (0%) and fully-injected channel (100%) for measured inductor	98
Figure 4.14	Inductance values at empty channel (0%) and fully-injected channel (100%) for measured inductor	98
Figure 4.15	Tuning range of the measured inductor	99
Figure 4.16	Quality factor comparison between simulations and measured results of the 400 MHz design inductor	101
Figure 4.17	Inductance values comparison between simulations and measured results of the 400 MHz design inductor	102
Figure 4.18	Comparison between simulated μ_r and measured values on the quality factor at 400 MHz	104
Figure 4.19	White marks on a surface of metal traces	105
Figure 4.20	Smith chart for S-parameters	106
Figure F.1	Two-port network with S-parameters model (Jamal Deen <i>et al.</i> , 2002)	
Figure F.2	The equivalent circuit of the inductor model with second-port shorted to the ground (Passos, 2013)	

- Figure F.3 π model of the inductor in Y-parameters (Okada *et al.*, 2010)
- Figure F.4 Shunt model of the inductor (Okada *et al.*, 2010)
- Figure G.1 E5071C ENA Network Analyzer
- Figure G.2 The connection of the male-to-male SMA cables to the network analyzer at port 1 and 2
- Figure G.3 GSG probe of 150 μm connected to the male-to-male SMA cables
- Figure G.4 Short, Open, and Load standard
- Figure G.5 Thru standard attached to the SMA cables
- Figure G.6 Correction coefficient of the Load standard in Smith chart and Log Mag
- Figure G.7 The 400 MHz design inductor before injection
- Figure G.8 The 400 MHz design inductor after injection
- Figure G.9 The 400 MHz design inductor measured under the microscope with injected ferrofluid-based

LIST OF ABBREVIATIONS

RFIC	Radio Frequency Integrated Circuit
RF	Radio Frequency
IC	Integrated Circuits
Si	Silicon
MEMS	Microelectronic Mechanical Systems
MMIC	Monolithic Microwave Integrated Circuits
UHF	Ultra-High Frequency
VCO	Voltage-Controlled Oscillator
LNA	Low-Noise Amplifier
IEEE	Institute of Electrical and Electronics Engineers
PCB	Printed Circuit Board
SOI	Silicon on Insulator
CMOS	Complementary Metal-Oxide-Semiconductor
3D	3-Dimensional
SiO ₂	Silicon Dioxide
SRF	Self-Resonance Frequency
PDMS	Polydimethylsiloxane
ABS	Acrylonitrile Butadiene Styrene
WLAN	Wireless Local Area Network
GSG	Ground Source Ground
RCA	Radio Corporation of America
AMI	Acetone-Methanol-Isopropanol
DC	Direct Current

CAD	Computer-Added Design
EFO	Electronic-Flame-Off
VNA	Vector Network Analyzer
SMA	SubMiniature version A
SOLT	Short-Open-Load-Thru

REKA BENTUK DAN PELAKSANAAN BERASASKAN BENDALIR BOLEH LARAS-HALUS PENGARUH MEMS SOLENOID

ABSTRAK

Peranti pasif seperti pengaruh litar bersepadu memainkan peranan penting dalam litar frekuensi radio. Walau bagaimanapun, prestasi kualiti faktor bagi pengaruh jenis ini dihadkan atas pengaruh substrat yang tinggi. Oleh itu, dalam tesis ini, bendalir boleh laras-halus pengaruh sistem mikroelektronik mekanikal solenoid dibentangkan untuk aplikasi frekuensi ultra tinggi. Bendalir Ferro berasaskan hidrokarbon ringan digunakan dalam reka bentuk untuk mencapai penalaan halus bagi nilai pengaruh. Tiub mikro bertindak sebagai saluran untuk penalaan. Tambahan daripada itu, teknik 'wire bonding' digunakan bagi tujuan mengurangkan rintangan siri, kehilangan substrat, dan kehilangan resonan sendiri. Wayar emas digunakan bagi mengikat bahagian pinggir dua pad logam. Ikatan dilakukan secara diagonal dengan menyeberangi bahagian atas tiub mikro. Pengaruh direka bentuk menggunakan ANSYS HFSS dan bacaan pengukuran ditetapkan pada frekuensi 400 MHz bagi tujuan pembuktian konsep. Pada frekuensi 400 MHz, keputusan simulasi menunjukkan kualiti faktor meningkat dari 10 hingga 12 manakala nilai pengaruh berubah dari 7.48 nH hingga 9.06 nH bagi saluran tiub kosong dan saluran tiub yang telah disuntik dengan bendalir Ferro. Keputusan menunjukkan julat penalaan sebanyak 21% berjaya dicapai. Namun demikian, keputusan bagi bacaan pengukuran pengaruh menunjukkan, pada frekuensi 400 MHz, nilai kualiti faktor secara perlahan menurun dari 6.79 kepada 5.49 dengan nilai pengaruh meningkat dari 21.40 nH kepada 22.40 nH bagi saluran tiub kosong dan saluran tiub yang telah disuntik dengan bendalir Ferro. Keputusan ini telah memberikan bacaan julat penalaan sebanyak 4.67%. Kesimpulannya, reka bentuk berasaskan bendalir boleh laras-halus pengaruh sistem mikroelektronik mekanikal solenoid berjaya dicapai untuk aplikasi frekuensi ultra tinggi.

DESIGN AND IMPLEMENTATION OF LIQUID-BASED FINE-TUNABLE SOLENOID MEMS INDUCTOR

ABSTRACT

Passive devices such as on-chip inductors play an important role in radio frequency circuits. However, these types of inductor lacked in terms of quality factor performance due to high substrate parasitic. Thus, in this thesis, liquid-based fine-tunable solenoid microelectronic mechanical systems inductor with high quality factor is presented for ultra-high frequency applications. The light hydrocarbon-based ferrofluid is utilised in the design to achieve a fine-tuning inductance. A micro-tube acts as a channel for tunability. In addition to that, wire bonding technique is applied to reduce series resistance, substrate loss, and self-resonance loss. A gold wire is bonded diagonally at the edge of metal pad by crossing it over the top of the micro-tube. The designed inductor was simulated using ANSYS HFSS and measured at a frequency of 400 MHz for proof-of-concept work. At 400 MHz, simulation results show that the quality factor increases from 10 to 12 with inductance values tuning from 7.48 nH to 9.06 nH for empty channel and fully-injected channel, respectively. Thus, tuning range of 21% is successfully achieved. The measured results however, reveals that, at 400 MHz, the quality factor gradually decreases from 6.79 to 5.49 with inductance values tuning from 21.40 nH to 22.40 nH for empty channel and fully-injected channel, respectively, giving a tuning range of 4.67%. In conclusion, the design of liquid-based fine-tunable solenoid microelectronic mechanical systems inductor is proven workable for ultra-high frequency applications.

CHAPTER ONE

INTRODUCTION

1.1 Introduction of Research

For years, integrated passive devices become a major topic in radio frequency integrated circuit (RFIC) applications. Integrated passive device such as inductor play a key role in radio frequency (RF) circuits. However, the miniaturization of the inductor along with integrated circuits (IC) are hard to realize (Gijs, 2008). Beside of having difficulties to reduce its size, the performance of integrated inductor such as quality factor is hard to achieve especially at GHz frequency. This is due to ohmic loss and eddy-current loss in a metal traces and substrate. Aside from that, a high substrate loss also appears in a bulk silicon (Si) substrate (Niknejad and Meyer, 2001). Therefore, studies have come out with a solution where a high frequency devices can be realized by applying microelectronic mechanical systems (MEMS) technologies into the inductor (Zhang *et al.*, 2010).

MEMS can be applied to the geometries of the inductor as an approach to improve quality factor. The quality factor performance can be improved through several techniques such as; maximizing the width of the conductor (Weon *et al.*, 2005); shrinking the size of inner turns (Lopez-Villegas, Samitier and Cane, 1998); distance the gap between segments of winding (Passos, 2013); embedding the inductor on the wafer (Sun and Miao, 2005), and back grinding the substrate (Han *et al.*, 2013). Besides, another best way to approach MEMS technology is by making the inductor tunable (Banitorfian *et al.*, 2013). One of the techniques that can be realized is by

changing the magnetic permeability of inductor core with a magnetic fluid i.e. ferrofluid (Banitorfian, 2016). A tunable MEMS inductor has a capability to tune a range of inductance values depending on the number of turns of the winding coils. Another interesting approach on MEMS inductor is by having Si wafer as the substrate of the device. This approach will completely open-up to a new discovery on the RFIC applications. Figure 1.1 show one example of the MEMS inductor (Yu *et al.*, 2014).

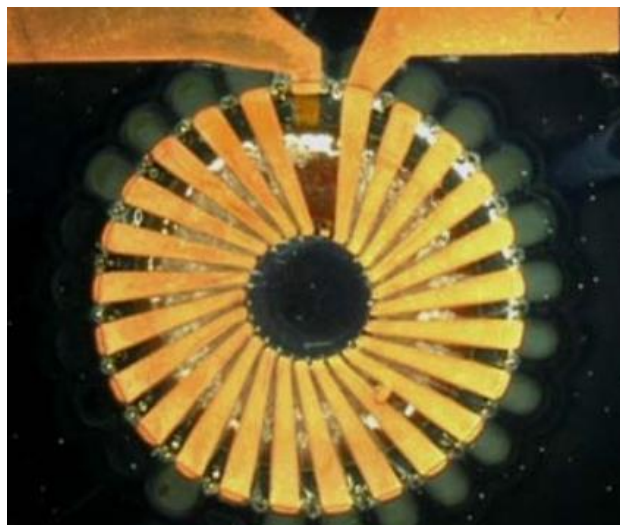


Figure 1.1: Silicon-embedded toroidal MEMS inductor (Yu *et al.*, 2014)

The MEMS inductor can be categorised into several types. These types of inductor are; solenoid, spiral, square, hexagonal, octagonal, toroidal, and meander. The best way to utilise inductance tuning is to use solenoid shape. This is due to less edge and corner effects on the solenoid type compared to others. The edge of metal conductor contributes more current distribution crowded on that area which increase the series resistance of the inductor (Banitorfian *et al.*, 2014). In addition, the solenoid type has an advantage on low substrate loss effect. This is due to only the bottom part of the solenoid is in direct contact with the substrate. Thus, a high quality factor can

easily be achieved with the solenoid shapes. Figure 1.2 show an example of the solenoid MEMS inductor (Seok *et al.*, 2001).

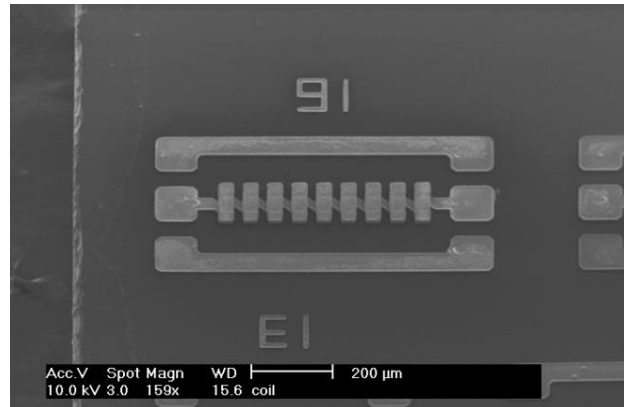


Figure 1.2: Solenoid MEMS inductor (Seok *et al.*, 2001)

1.2 Problem Statement

The demands on low-cost fabrication with high-performance on-chip RFIC applications are strongly needed today. Conventionally, on-chip monolithic microwave integrated circuits (MMIC) inductor are integrated with a standard silicon substrate and aluminium as a metal interconnects (Zaki, 2006). This low-cost on-chip inductor exhibit poor quality factor due to the substrate parasitic and ohmic losses in aluminium traces. Moreover, the MMIC inductor cannot be made tunable. For that matter, several solutions have been made to increase the quality factor of the devices and at the same time to make it tunable. Therefore, the MEMS inductor is utilised in this work for achieving high-performance integrated inductor.

In previous work, several methods were implemented to improve quality factor. Most of the inductor designed by previous researchers were said to achieve a

good quality factor performance. However, most of them do not have a tuning capability. Such examples can be seen in (Chomnawang and Lee, 2001), (Weon *et al.*, 2005), and (Pólik and Kuczmann, 2010), where quality factors observed are more than 30 but do not have tuning capability. Following these work, inductors with tuning capability were introduced to add values to the high quality factor performance of the inductor (Banitorfian *et al.*, 2015) and (Banitorfian *et al.*, 2016). Unfortunately, the proposed designs are not dedicated for 2.4 GHz range of application, where wireless communication devices such as routers or mobile phones normally operate.

In work (Banitorfian *et al.*, 2015) and (Banitorfian *et al.*, 2016), the operating frequencies were recorded at 4 GHz and 0.15 GHz. As observed, this operating frequencies were way off the proposed design of 2.4 GHz. The problem of tuning the operating frequency to 2.4 GHz was due to the size constraint of the inductor. For example, (Banitorfian *et al.*, 2016) was only recorded as proof-of-concept work due to smaller inductor design was not achievable. This resulted has led (Banitorfian *et al.*, 2016) work to only capable operating at frequency of 0.15 GHz. However, in work (Banitorfian *et al.*, 2015), the design was recorded as a simulation inductor which a high frequency of 4 GHz can easily be achieved. Thus, to ensure the inductor can be fabricated, operating frequency is need be limited to 400 MHz as a proof-of-concept, considering that low operating frequency of less than 500 MHz can only be achieved with inductor size of more than 1 mm.